forces and response functions in QMC

Saverio Moroni
SISSA and DEMOCRITOS, IOM-CNR, Trieste, Italy

1) minimum energy pathways:
a black-box calculation with QMC forces

2) imaginary-time correlation functions:
unbiased fermionic energies, static and dynamic response

with: S. Saccani, C. Filippi, E. Vitali, M. Nava, M.Motta, D. Galli,
M. Taddei, M. Holzmann

1) minimum energy pathways:
a black-box calculation with QMC forces

- variational and Fixed-node diffusion Monte Carlo

- forces in QMC and optimization of the trial function

- test on reaction paths of small molecules:
  - reasonably automatic
  - reasonably accurate (wrt. DFT)
  - presumably scalable to large systems

- improving the trial function

Energy derivatives in QMC:

$$E = \int E_L P dX / Z = \langle E_L \rangle$$

$$E' = \langle E'_L + (E_L - E)(\ln P)' \rangle$$

$$E'' = \langle E''_L + (E_L - E)(\ln P)''$$

$$+(E_L - E)(\ln P)'(\ln P)' + 2(E'_L - E')(\ln P)' \rangle$$

$P = \Psi^2$ Variational Monte Carlo

$P = \Psi \Phi_{FN}$ Fixed-node QMC

these estimators have the zero-variance property

but their variance is actually infinite...

Energy derivatives in QMC: a toy problem

1D particle in a box, $H = -\frac{1}{2}\frac{\partial^2}{\partial x^2} + \gamma x, \qquad -L < x < L$

Trial function (wrong on purpose): $\Psi_T(x) = \cos(kx)(1 + \alpha x)$

data trace:

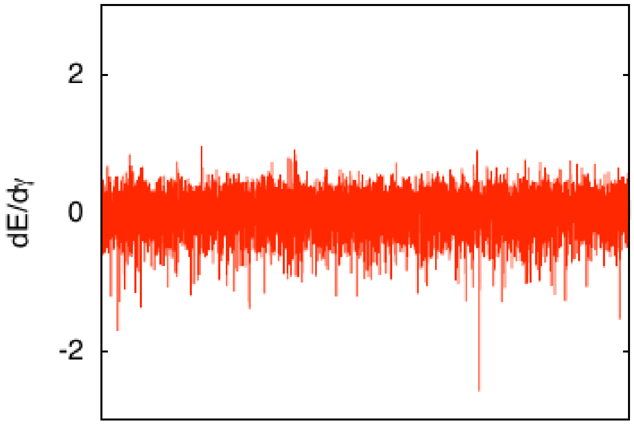

$$\frac{dE}{d\gamma}$$

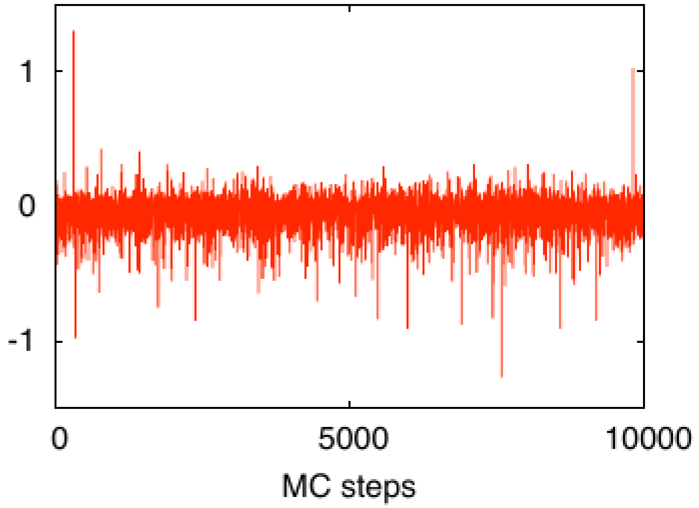

$$\frac{d^2E}{d\gamma^2}$$

This is a “bosonic” case; the variance is finite

Energy derivatives in QMC: a toy problem

1D particle in a box, $H = -\frac{1}{2}\frac{\partial^2}{\partial x^2} + \gamma x, \qquad -L < x < L$

Trial function (wrong on purpose): $\Psi_T(x) = \cos(kx)(1+\alpha x)$

data trace:

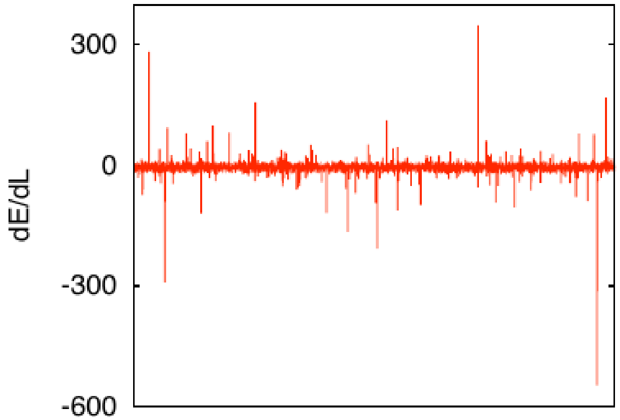

$$\frac{dE}{dL}$$

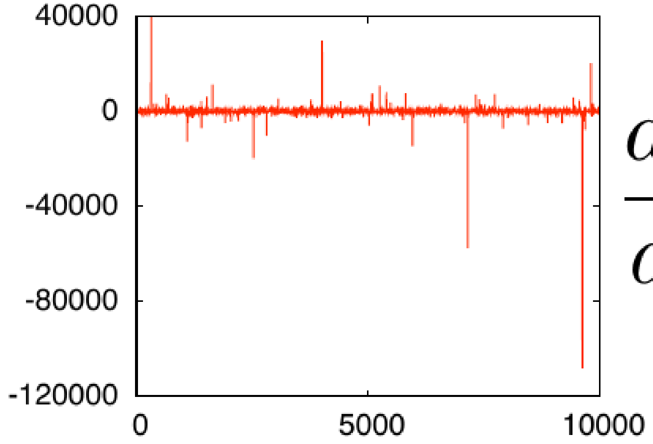

$$\frac{d^2E}{dL^2}$$

This is a “fermionic” case; the variance is infinite

Energy derivatives in QMC

$$E' = \int \left[E_L' + (E_L - E)(\ln P)'\right] P dX/Z$$

near a node:

$$E_L \sim 1/d, \qquad d = |\Psi_T / \nabla \Psi_T| \quad \text{nodal distance}$$

$$E_L' \sim 1/d^2$$

$$P \sim d^2$$

the integral of PE_L' is bounded,

but the integral of $P(E_L')^2$ is not.

→ infinite variance

Finite-variance derivatives in QMC (Attaccalite, Sorella 2008)

sample the square of a guiding function finite at the nodes (VMC)

(an equivalent trick is possible in DMC as well)

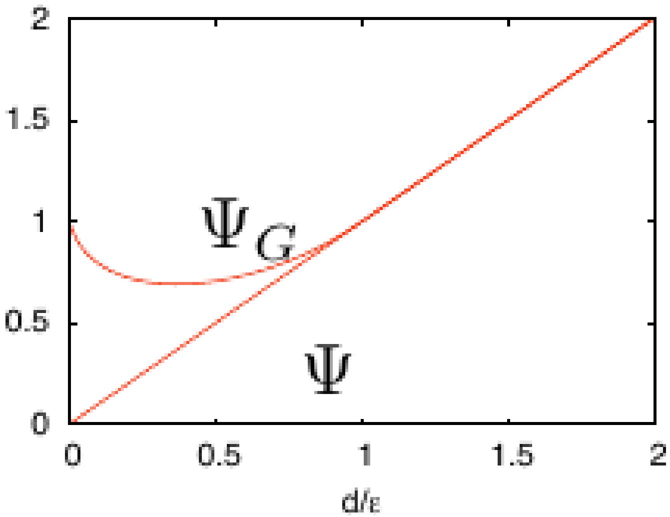

$$E' = \frac{\int \left[E_L' + (E_L - E)(\ln P)'\right] W P_G dX}{\int W P_G dX}$$

$$P_G \sim \text{const}, \qquad W = P/P_G \sim d^2, \qquad E_L' W \sim \text{const}$$

→ the variance is finite

Energy derivatives in QMC: a toy problem

1D particle in a box, $H = -\frac{1}{2}\frac{\partial^2}{\partial x^2} + \gamma x, \qquad -L < x < L$

Trial function (wrong on purpose): $\Psi_T(x) = \cos(kx)(1 + \alpha x)$

data trace:

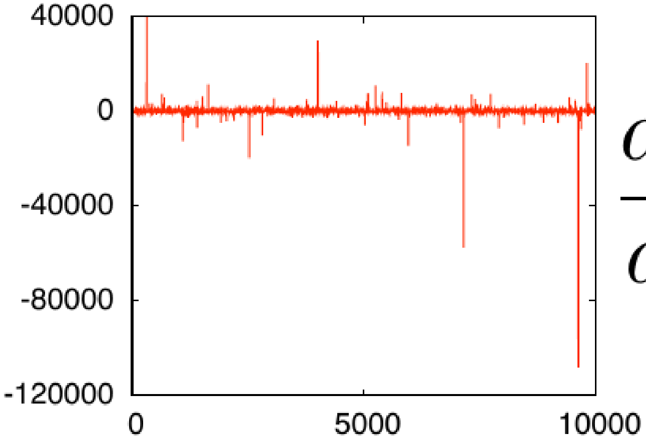

$$\frac{d^2 E}{dL^2}$$

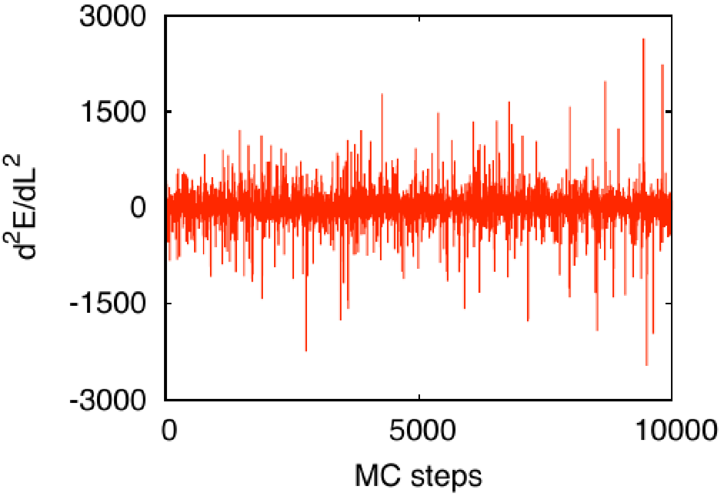

regularized

The variance is now finite (but still large...)

low-variance derivatives in FN-DMC (Filippi, Umrigar 2000):

DMC samples $\prod_{i=1}^{k} G_{dd}(R_i, R_{i-1}) e^{-\tau[E_L(R_i)+E_L(R_{i-1})]/2}$

The drift-diffusion term G_{dd} gives high statistical noise in the calculation of derivatives.

Replace $\nabla \prod_{i=1}^{k} G_{dd}(R_i, R_{i-1}) \rightarrow \nabla \Psi_T^2(R_k)$

This estimator is approximate but accurate (if Ψ_T is exact the branching term is a constant and $\prod G_{dd}$ just samples Ψ_T^2).

forces as partial derivatives:

$$\frac{dE}{d\lambda} = \frac{\partial E}{\partial \lambda} + \sum_i \frac{\partial E}{\partial c_i}\frac{\partial c_i}{\partial \lambda}$$

c_i variational parameters in Ψ_T

Optimize* all variational parameters $\rightarrow \frac{dE}{d\lambda} = \frac{\partial E}{\partial \lambda}$

In the following results for reactions, optimization and calculation of forces take approximately the same CPU time.

*C.J.Umrigar, J.Toulouse, C.Filippi, S.Sorella and R.G.Hennig,
PRL 98, 110201 (2007).

Wave function optimization by energy minimization (Umrigar, Toulouse, Filippi, Sorella, Hennig 2007).

- consider the space spanned by the wave function and its derivatives with respect to the variational parameters c_i:

$$\Psi_i = \partial\Psi/\partial c_i, \quad i > 1; \qquad \Psi_0 = \Psi; \qquad \Omega = \{\Psi_i\}$$

- linear method: find lowest-energy eigenstate in Ω solving

$$\sum \langle\Psi_i|H|\Psi_j\rangle x_j = E \sum \langle\Psi_i|H|\Psi_k\rangle x_k$$

- update variational parameters $c_i' = c_i + x_i/x_0$

Example (Neuscamman, Umrigar, Chen 2012):
~10000 parameters for free-base porphirine

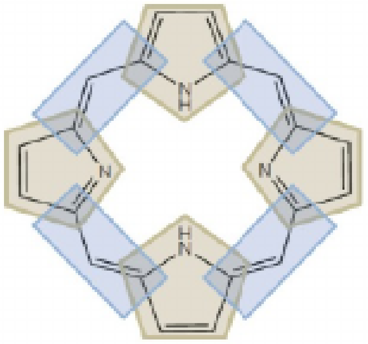

Test of force as partial derivative in VMC: Carbon dimer

$$H = -\frac{1}{2}\sum_i \nabla_i^2 - \sum_{i,A} \frac{Z_A}{r_{iA}} + \sum_{i<j} \frac{1}{r_{ij}}$$

$$\Psi_T(R) = J(R)D(R)$$

$J(R)$ symmetric Jastrow factor with e-e, e-n and e-e-n correlation

$D(R) = \det(\phi_i(\mathbf{r}_j))$ Slater determinant of single-particle orbitals

$\phi_i(\mathbf{r}_j) = \sum_\alpha c_{i\alpha}\chi_\alpha(\mathbf{r}_j)$ orbitals expanded in a basis set

Test of force as partial derivative in VMC: Carbon dimer

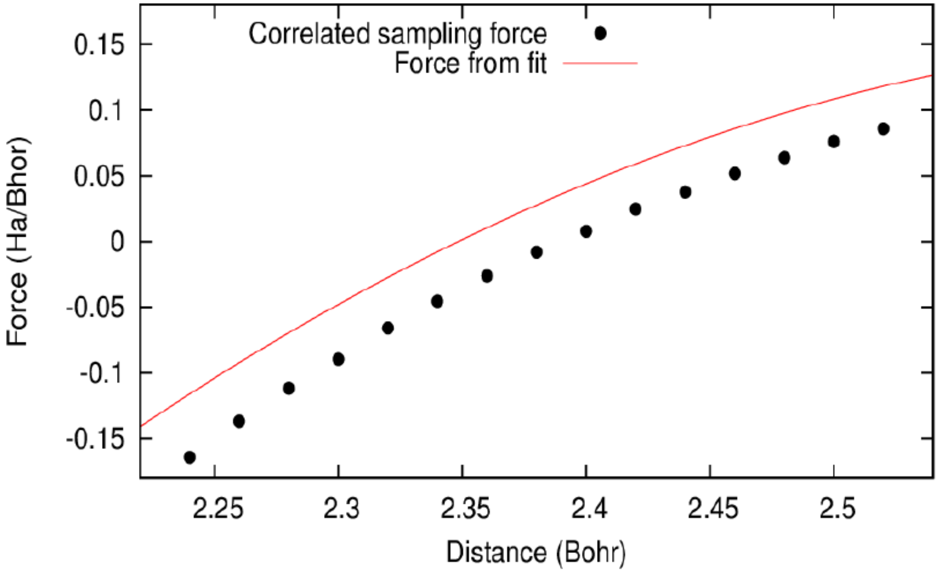

HF orbitals,
optimized Jastrow

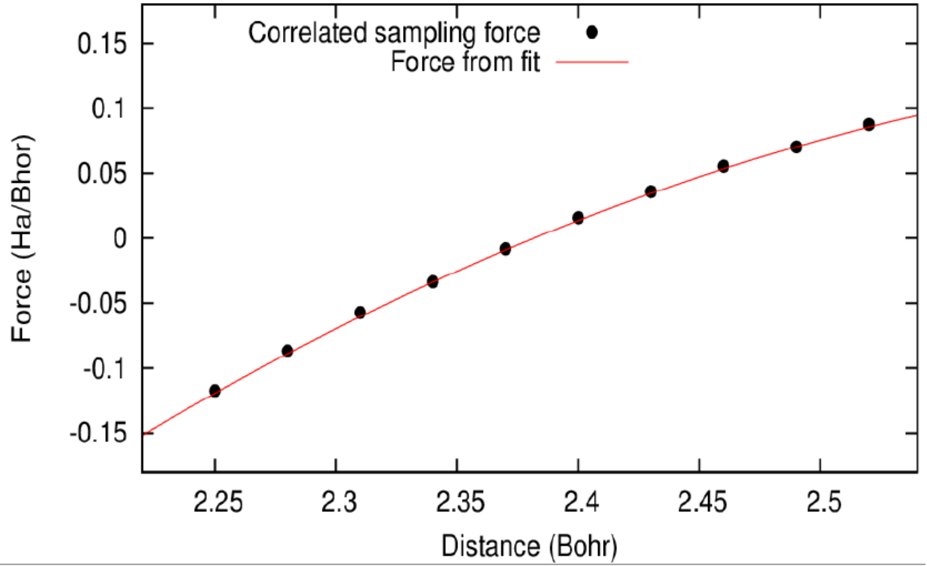

optimized orbitals,
optimized Jastrow

Test of approximation to DMC forces: Carbon dimer

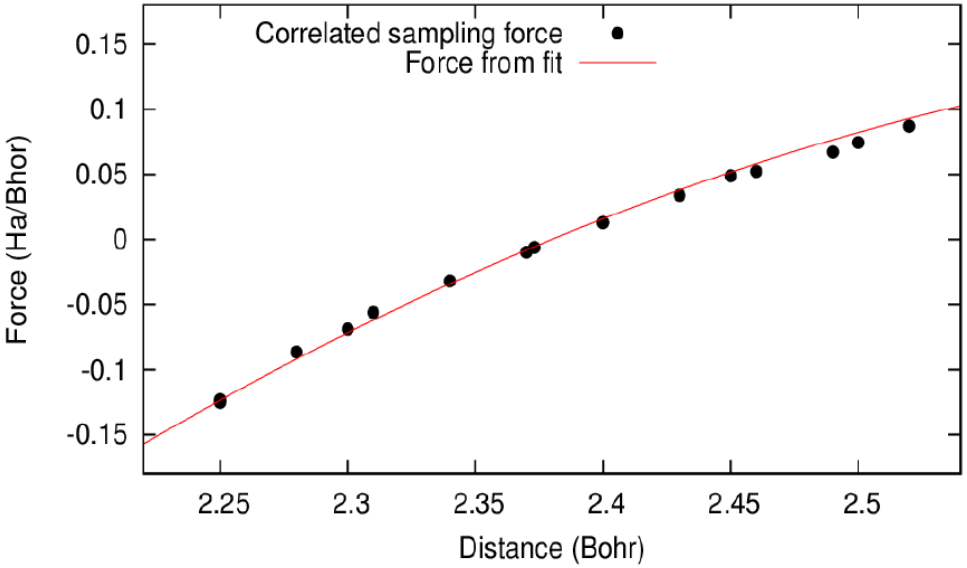

DMC forces with replacement $\nabla \prod_{i=1}^{k} G_{dd}(R_i, R_{i-1}) \rightarrow \nabla \Psi_T^2(R_k)$

Accuracy of FN-DMC for molecular systems:

DMC atomization energies for the G2 data set (Petruzielo, Toulouse, Umrigar 2012)

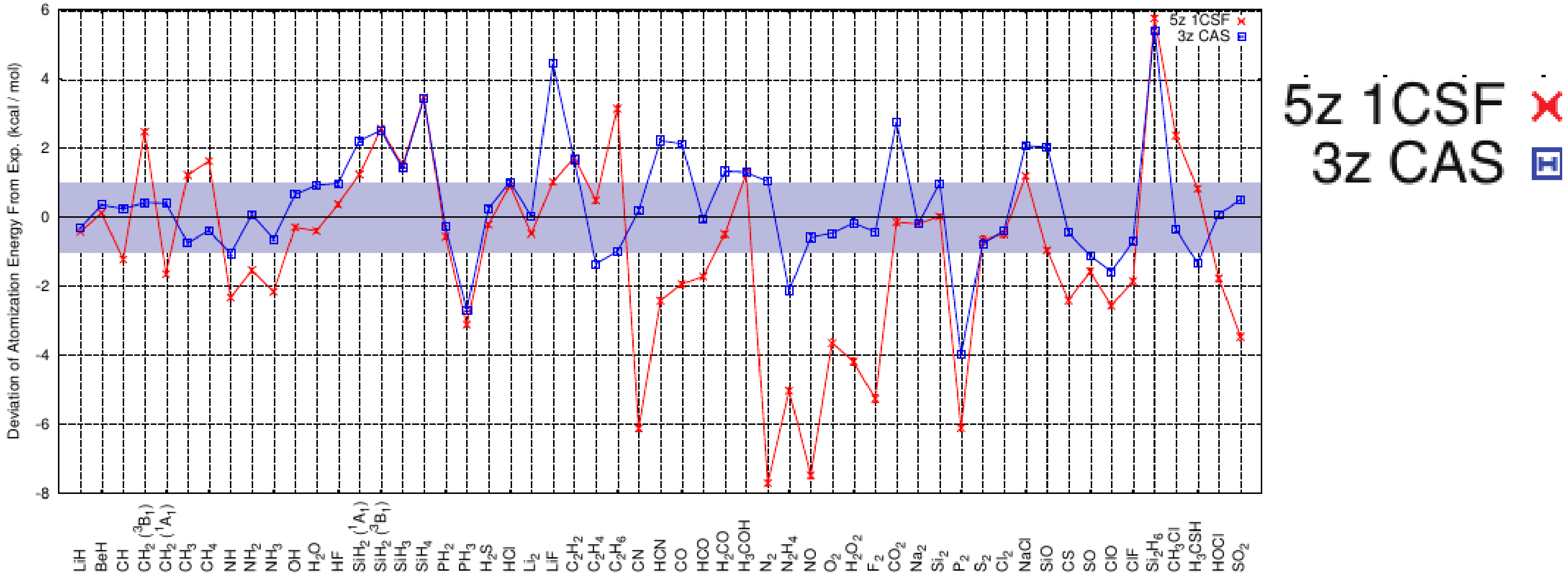

Fixed-node DMC with multideterminant wavefunction approaches chemical accuracy:

wavefunction	HF orbitals	optimized orbitals	CAS
MAD (kcal/mol)	3.0	2.1	1.2

- For scalability we will use 2z one-determinant SJ wavefunction
- Expected accuracy ~a few kcal/mol: is that enough?

Nudged Elastic Band: a method to find minimum-energy paths

Extensively used for catalysis problems,
mostly within DFT (especially GGA)

$$\begin{aligned}\mathbf{F}_\perp &= \left(\mathbf{F}\cdot\mathbf{n}_\perp\right)\mathbf{n}_\perp \\ \mathbf{F}_\parallel &= \left(\mathbf{F_s}\cdot\mathbf{n}_\parallel\right)\mathbf{n}_\parallel\end{aligned}$$

After convergence,
find transition state by
climbing image:

$$\begin{aligned}\mathbf{F}_\perp &= \left(\mathbf{F}\cdot\mathbf{n}_\perp\right)\mathbf{n}_\perp \\ \mathbf{F}_\parallel &= -\left(\mathbf{F}\cdot\mathbf{n}_\parallel\right)\mathbf{n}_\parallel\end{aligned}$$

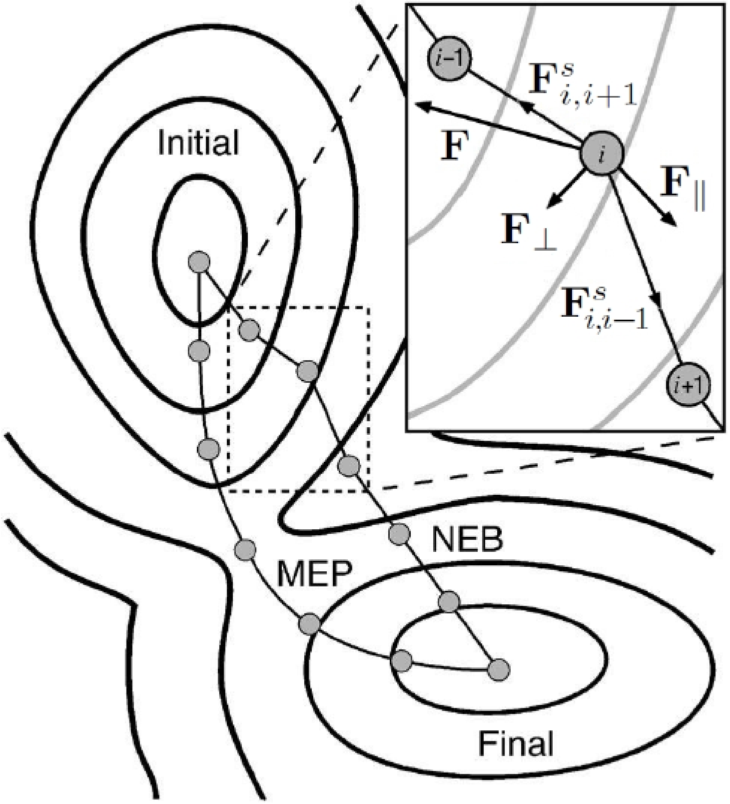

G.Henkelman, B.P.Uberuaga, and H.Jonsson, JCP 113, 9901 (2000)

Y.Zhao, N.Gonzalez-Garcia, and D.G.Truhlar, JPC A 109, 2012 (2005)

Barrier heigths calculated by LSDA, GGA and Meta DFT methods:

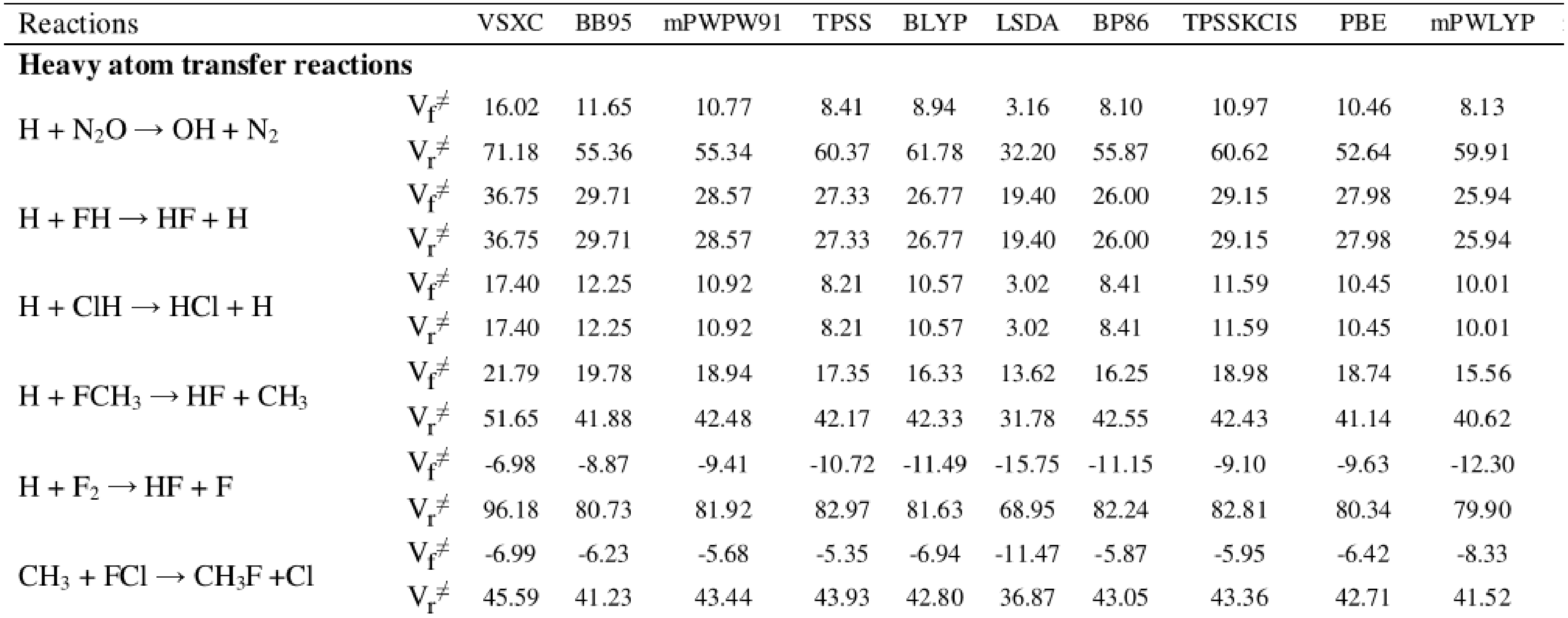

Reactions		VSXC	BB95	mPWPW91	TPSS	BLYP	LSDA	BP86	TPSSKCIS	PBE	mPWLYP
Heavy atom transfer reactions											
$H + N_2O \rightarrow OH + N_2$	$V_f^{\neq}$	16.02	11.65	10.77	8.41	8.94	3.16	8.10	10.97	10.46	8.13
	$V_r^{\neq}$	71.18	55.36	55.34	60.37	61.78	32.20	55.87	60.62	52.64	59.91
$H + FH \rightarrow HF + H$	$V_f^{\neq}$	36.75	29.71	28.57	27.33	26.77	19.40	26.00	29.15	27.98	25.94
	$V_r^{\neq}$	36.75	29.71	28.57	27.33	26.77	19.40	26.00	29.15	27.98	25.94
$H + ClH \rightarrow HCl + H$	$V_f^{\neq}$	17.40	12.25	10.92	8.21	10.57	3.02	8.41	11.59	10.45	10.01
	$V_r^{\neq}$	17.40	12.25	10.92	8.21	10.57	3.02	8.41	11.59	10.45	10.01
$H + FCH_3 \rightarrow HF + CH_3$	$V_f^{\neq}$	21.79	19.78	18.94	17.35	16.33	13.62	16.25	18.98	18.74	15.56
	$V_r^{\neq}$	51.65	41.88	42.48	42.17	42.33	31.78	42.55	42.43	41.14	40.62
$H + F_2 \rightarrow HF + F$	$V_f^{\neq}$	-6.98	-8.87	-9.41	-10.72	-11.49	-15.75	-11.15	-9.10	-9.63	-12.30
	$V_r^{\neq}$	96.18	80.73	81.92	82.97	81.63	68.95	82.24	82.81	80.34	79.90
$CH_3 + FCl \rightarrow CH_3F + Cl$	$V_f^{\neq}$	-6.99	-6.23	-5.68	-5.35	-6.94	-11.47	-5.87	-5.95	-6.42	-8.33
	$V_r^{\neq}$	45.59	41.23	43.44	43.93	42.80	36.87	43.05	43.36	42.71	41.52

Part of one of the tables for the NHTBH38/04 database

Y.Zhao, N.Gonzalez-Garcia, and D.G.Truhlar, JPC A 109, 2012 (2005)

Barrier heigths calculated by LSDA, GGA and Meta DFT methods:

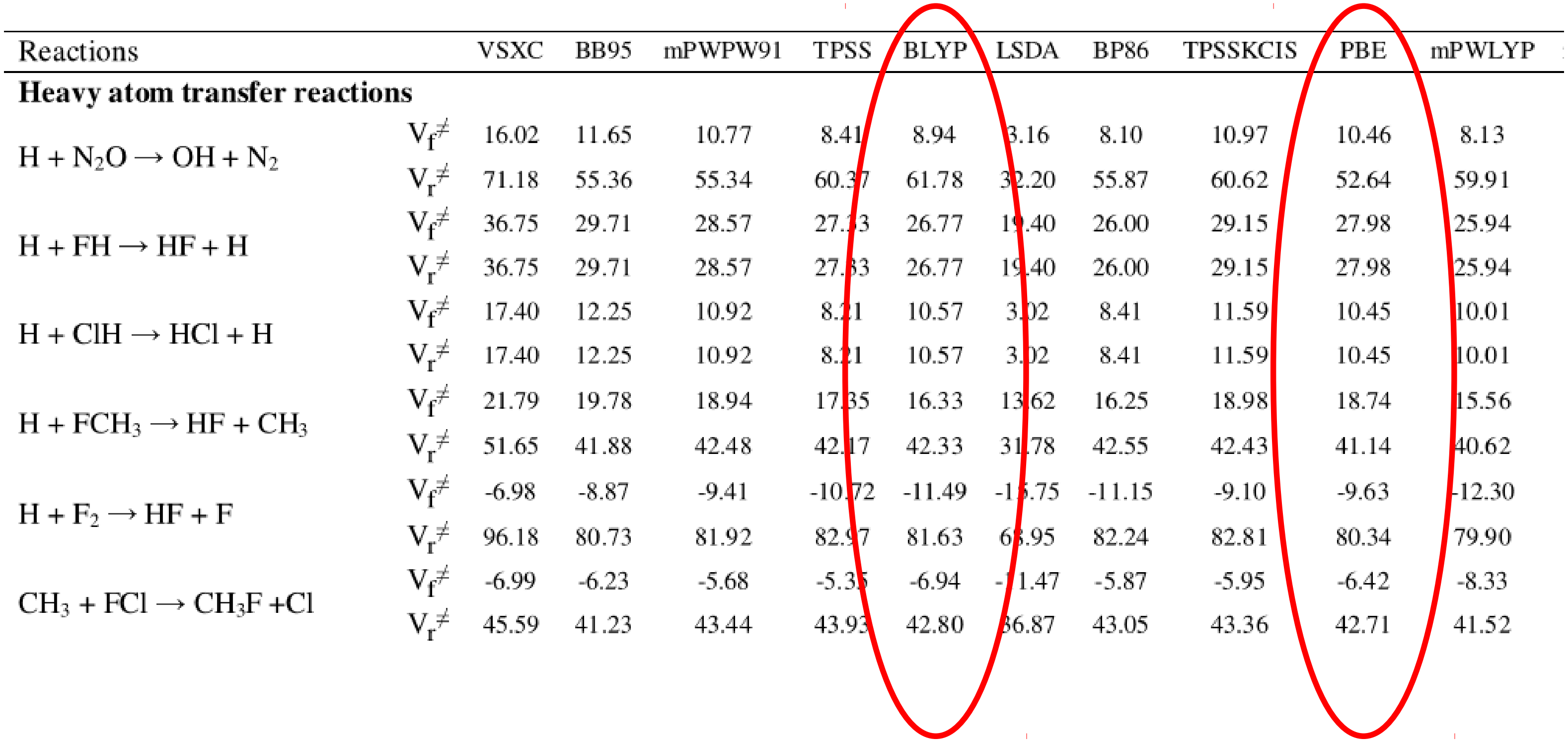

Reactions		VSXC	BB95	mPWPW91	TPSS	BLYP	LSDA	BP86	TPSSKCIS	PBE	mPWLYP
Heavy atom transfer reactions											
$H + N_2O \rightarrow OH + N_2$	$V_f^{\neq}$	16.02	11.65	10.77	8.41	8.94	3.16	8.10	10.97	10.46	8.13
	$V_r^{\neq}$	71.18	55.36	55.34	60.37	61.78	32.20	55.87	60.62	52.64	59.91
$H + FH \rightarrow HF + H$	$V_f^{\neq}$	36.75	29.71	28.57	27.33	26.77	19.40	26.00	29.15	27.98	25.94
	$V_r^{\neq}$	36.75	29.71	28.57	27.33	26.77	19.40	26.00	29.15	27.98	25.94
$H + ClH \rightarrow HCl + H$	$V_f^{\neq}$	17.40	12.25	10.92	8.21	10.57	3.02	8.41	11.59	10.45	10.01
	$V_r^{\neq}$	17.40	12.25	10.92	8.21	10.57	3.02	8.41	11.59	10.45	10.01
$H + FCH_3 \rightarrow HF + CH_3$	$V_f^{\neq}$	21.79	19.78	18.94	17.35	16.33	13.62	16.25	18.98	18.74	15.56
	$V_r^{\neq}$	51.65	41.88	42.48	42.17	42.33	31.78	42.55	42.43	41.14	40.62
$H + F_2 \rightarrow HF + F$	$V_f^{\neq}$	-6.98	-8.87	-9.41	-10.72	-11.49	-15.75	-11.15	-9.10	-9.63	-12.30
	$V_r^{\neq}$	96.18	80.73	81.92	82.97	81.63	68.95	82.24	82.81	80.34	79.90
$CH_3 + FCl \rightarrow CH_3F + Cl$	$V_f^{\neq}$	-6.99	-6.23	-5.68	-5.35	-6.94	-11.47	-5.87	-5.95	-6.42	-8.33
	$V_r^{\neq}$	45.59	41.23	43.44	43.93	42.80	36.87	43.05	43.36	42.71	41.52

Mean error: -14.66 -14.93

Y.Zhao, N.Gonzalez-Garcia, and D.G.Truhlar, JPC A 109, 2012 (2005)

Barrier heigths calculated by LSDA, GGA and Meta DFT methods:

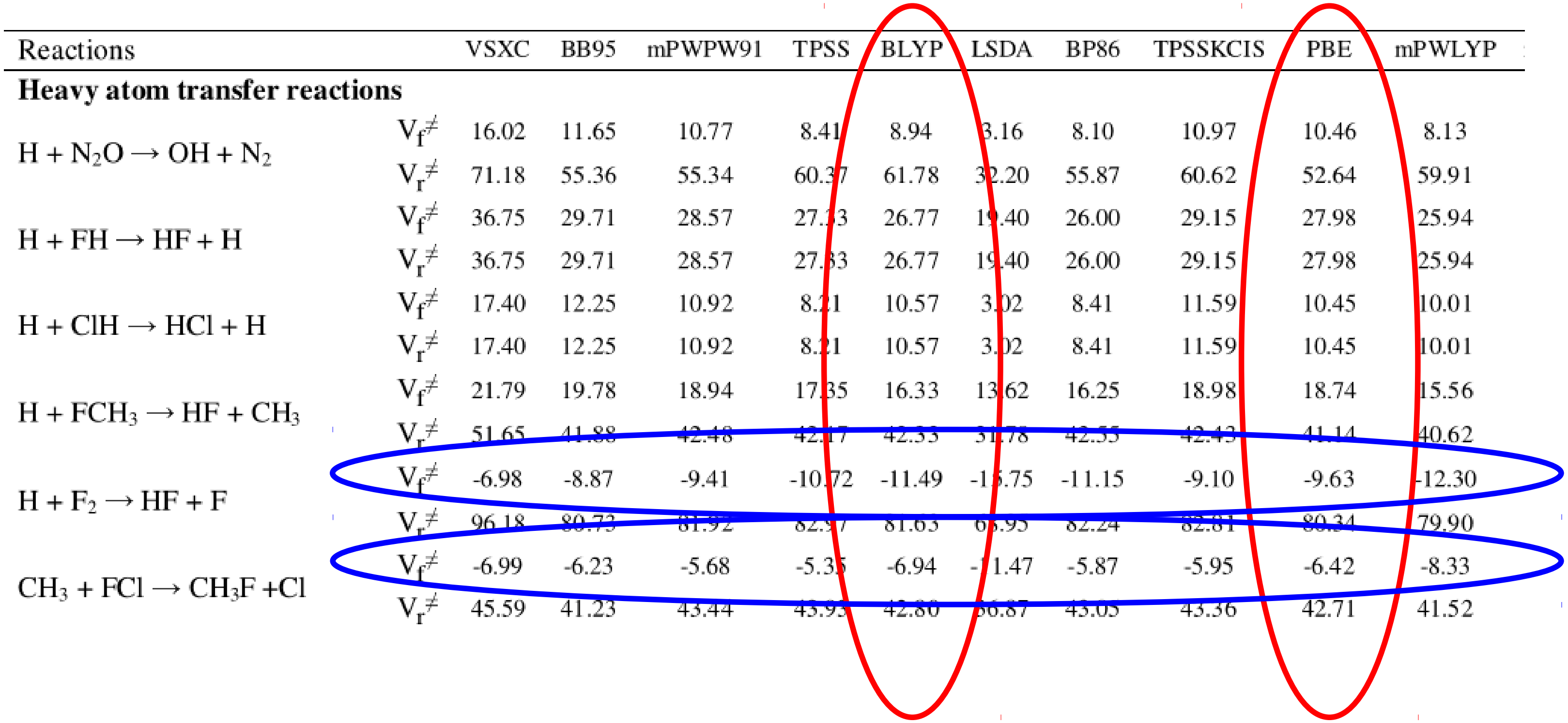

Reactions		VSXC	BB95	mPWPW91	TPSS	BLYP	LSDA	BP86	TPSSKCIS	PBE	mPWLYP
Heavy atom transfer reactions											
$H + N_2O \rightarrow OH + N_2$	$V_f^{\neq}$	16.02	11.65	10.77	8.41	8.94	3.16	8.10	10.97	10.46	8.13
	$V_r^{\neq}$	71.18	55.36	55.34	60.37	61.78	32.20	55.87	60.62	52.64	59.91
$H + FH \rightarrow HF + H$	$V_f^{\neq}$	36.75	29.71	28.57	27.33	26.77	19.40	26.00	29.15	27.98	25.94
	$V_r^{\neq}$	36.75	29.71	28.57	27.33	26.77	19.40	26.00	29.15	27.98	25.94
$H + ClH \rightarrow HCl + H$	$V_f^{\neq}$	17.40	12.25	10.92	8.21	10.57	3.02	8.41	11.59	10.45	10.01
	$V_r^{\neq}$	17.40	12.25	10.92	8.21	10.57	3.02	8.41	11.59	10.45	10.01
$H + FCH_3 \rightarrow HF + CH_3$	$V_f^{\neq}$	21.79	19.78	18.94	17.35	16.33	13.62	16.25	18.98	18.74	15.56
	$V_r^{\neq}$	51.65	41.88	42.48	42.17	42.33	31.78	42.55	42.43	41.14	40.62
$H + F_2 \rightarrow HF + F$	$V_f^{\neq}$	-6.98	-8.87	-9.41	-10.72	-11.49	-16.75	-11.15	-9.10	-9.63	-12.30
	$V_r^{\neq}$	96.18	80.73	81.92	82.97	81.63	66.95	82.24	82.81	80.34	79.90
$CH_3 + FCl \rightarrow CH_3F + Cl$	$V_f^{\neq}$	-6.99	-6.23	-5.68	-5.35	-6.94	-11.47	-5.87	-5.95	-6.42	-8.33
	$V_r^{\neq}$	45.59	41.23	43.44	43.93	42.80	56.87	43.05	43.36	42.71	41.52

Mean error: -14.66 -14.93

QMC calculation:

- Reactions studied [S.Saccani, C.Filippi and SM, JCP 138, 084109 (2013)]

H transfer: $H + OH \rightarrow H_2 + O$

Heavy atom transfer: $H + N_2O \rightarrow OH + N_2$

$H + F_2 \rightarrow HF + F$

Nucleophilic substitution: $F^- \cdots CH_3F \rightarrow FCH_3 \cdots F$

Association reaction: $H + CO \rightarrow HCO$

- Initial one-particle orbitals from GAMESS
- Pseudopotentials and optimized GTO VDZ basis from BFD*
- QMC energy and force calculations with CHAMP

* M.Burkatzki, C.Filippi and M. Dolg, JCP 126, 234105 (2007)

QMC results: Mean Unsigned Deviation from best estimates

forward barrier:

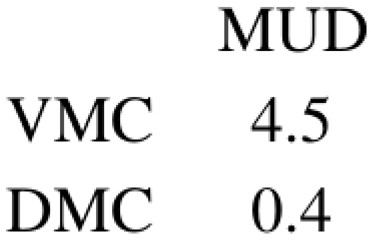

	MUD
VMC	4.5
DMC	0.4

reverse barrier:

VMC	8.1
DMC	3.0

Significant improvement over GGA DFT

...but there exist better functionals

Y.Zhao, N.Gonzalez-Garcia, and D.G.Truhlar, JPC A 109, 2012 (2005)

Barrier heigths calculated by hybrid methods:

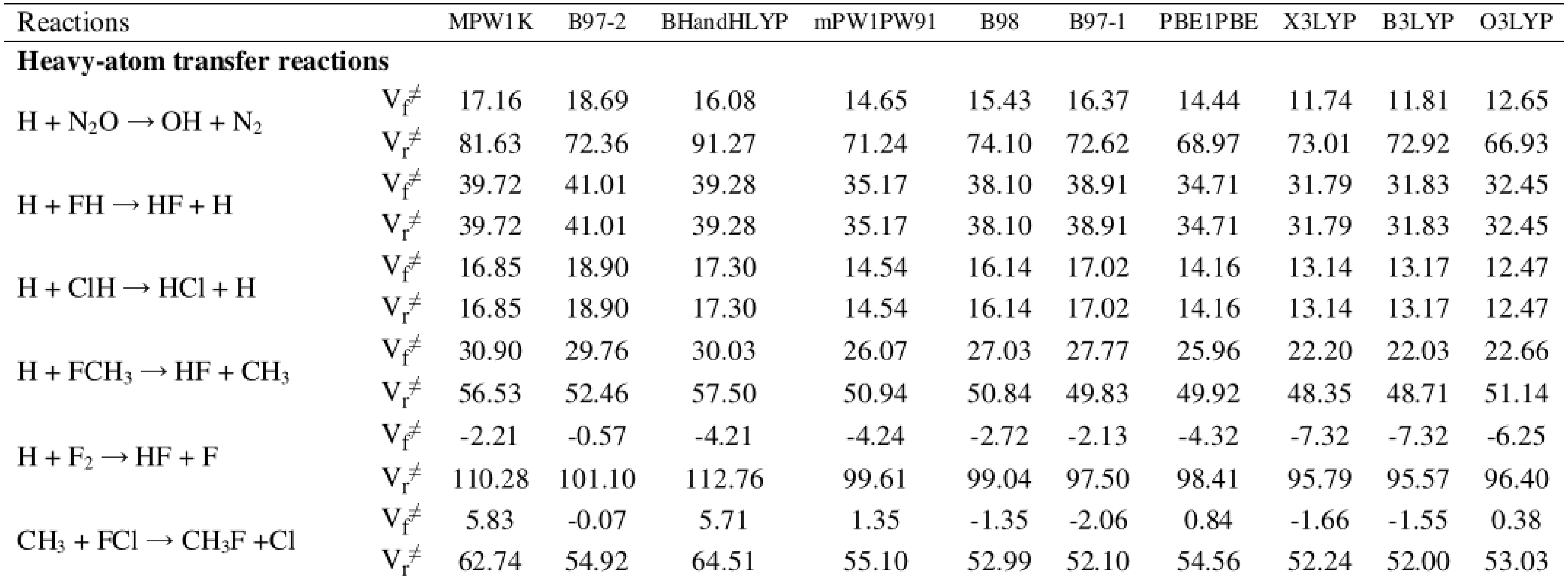

Reactions		MPW1K	B97-2	BHandHLYP	mPW1PW91	B98	B97-1	PBE1PBE	X3LYP	B3LYP	O3LYP
Heavy-atom transfer reactions											
$H + N_2O \rightarrow OH + N_2$	$V_f^{\neq}$	17.16	18.69	16.08	14.65	15.43	16.37	14.44	11.74	11.81	12.65
	$V_r^{\neq}$	81.63	72.36	91.27	71.24	74.10	72.62	68.97	73.01	72.92	66.93
$H + FH \rightarrow HF + H$	$V_f^{\neq}$	39.72	41.01	39.28	35.17	38.10	38.91	34.71	31.79	31.83	32.45
	$V_r^{\neq}$	39.72	41.01	39.28	35.17	38.10	38.91	34.71	31.79	31.83	32.45
$H + ClH \rightarrow HCl + H$	$V_f^{\neq}$	16.85	18.90	17.30	14.54	16.14	17.02	14.16	13.14	13.17	12.47
	$V_r^{\neq}$	16.85	18.90	17.30	14.54	16.14	17.02	14.16	13.14	13.17	12.47
$H + FCH_3 \rightarrow HF + CH_3$	$V_f^{\neq}$	30.90	29.76	30.03	26.07	27.03	27.77	25.96	22.20	22.03	22.66
	$V_r^{\neq}$	56.53	52.46	57.50	50.94	50.84	49.83	49.92	48.35	48.71	51.14
$H + F_2 \rightarrow HF + F$	$V_f^{\neq}$	-2.21	-0.57	-4.21	-4.24	-2.72	-2.13	-4.32	-7.32	-7.32	-6.25
	$V_r^{\neq}$	110.28	101.10	112.76	99.61	99.04	97.50	98.41	95.79	95.57	96.40
$CH_3 + FCl \rightarrow CH_3F + Cl$	$V_f^{\neq}$	5.83	-0.07	5.71	1.35	-1.35	-2.06	0.84	-1.66	-1.55	0.38
	$V_r^{\neq}$	62.74	54.92	64.51	55.10	52.99	52.10	54.56	52.24	52.00	53.03

Mean unsigned error: 1.58 11.51

Y.Zhao, N.Gonzalez-Garcia, and D.G.Truhlar, JPC A 109, 2012 (2005)

Barrier heigths calculated by hybrid methods:

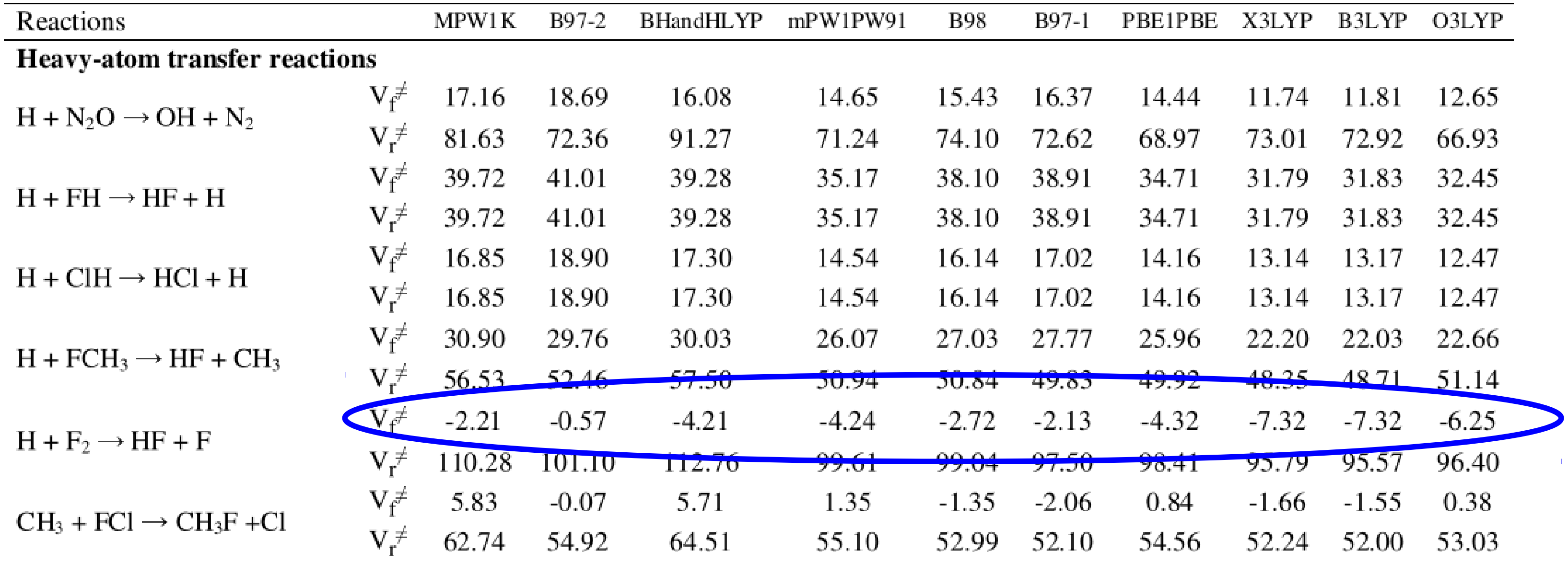

Reactions		MPW1K	B97-2	BHandHLYP	mPW1PW91	B98	B97-1	PBE1PBE	X3LYP	B3LYP	O3LYP
Heavy-atom transfer reactions											
$H + N_2O \rightarrow OH + N_2$	$V_f^{\neq}$	17.16	18.69	16.08	14.65	15.43	16.37	14.44	11.74	11.81	12.65
	$V_r^{\neq}$	81.63	72.36	91.27	71.24	74.10	72.62	68.97	73.01	72.92	66.93
$H + FH \rightarrow HF + H$	$V_f^{\neq}$	39.72	41.01	39.28	35.17	38.10	38.91	34.71	31.79	31.83	32.45
	$V_r^{\neq}$	39.72	41.01	39.28	35.17	38.10	38.91	34.71	31.79	31.83	32.45
$H + ClH \rightarrow HCl + H$	$V_f^{\neq}$	16.85	18.90	17.30	14.54	16.14	17.02	14.16	13.14	13.17	12.47
	$V_r^{\neq}$	16.85	18.90	17.30	14.54	16.14	17.02	14.16	13.14	13.17	12.47
$H + FCH_3 \rightarrow HF + CH_3$	$V_f^{\neq}$	30.90	29.76	30.03	26.07	27.03	27.77	25.96	22.20	22.03	22.66
	$V_r^{\neq}$	56.53	52.46	57.50	50.94	50.84	49.83	49.92	48.35	48.71	51.14
$H + F_2 \rightarrow HF + F$	$V_f^{\neq}$	-2.21	-0.57	-4.21	-4.24	-2.72	-2.13	-4.32	-7.32	-7.32	-6.25
	$V_r^{\neq}$	110.28	101.10	112.76	99.61	99.04	97.50	98.41	95.79	95.57	96.40
$CH_3 + FCl \rightarrow CH_3F + Cl$	$V_f^{\neq}$	5.83	-0.07	5.71	1.35	-1.35	-2.06	0.84	-1.66	-1.55	0.38
	$V_r^{\neq}$	62.74	54.92	64.51	55.10	52.99	52.10	54.56	52.24	52.00	53.03

Mean unsigned error: 1.58 11.51

QMC results: geometries for the reaction $H + F_2 \rightarrow HF + F$

Root mean square deviation of all interatomic distances from best estimate in $\mathring{A}$

	VMC	DMC	BLYP	PBE	B3LYP	PBE0	M06
React	0.008	0.007	0.037	0.018	0.002	0.019	0.020
Prod	0.002	0.008	0.029	0.017	0.009	0.004	0.001
TS	0.028	0.013	-	-	-	-	0.216

- Within DFT only the M06 functional* does find a barrier
- VMC improves the geometry of the transition state significantly
- Further geometrical improvement with DMC is marginal

*constructed to fit (also) accurate barrier heights for the NHTBH38/04 database

QMC vs DFT geometries

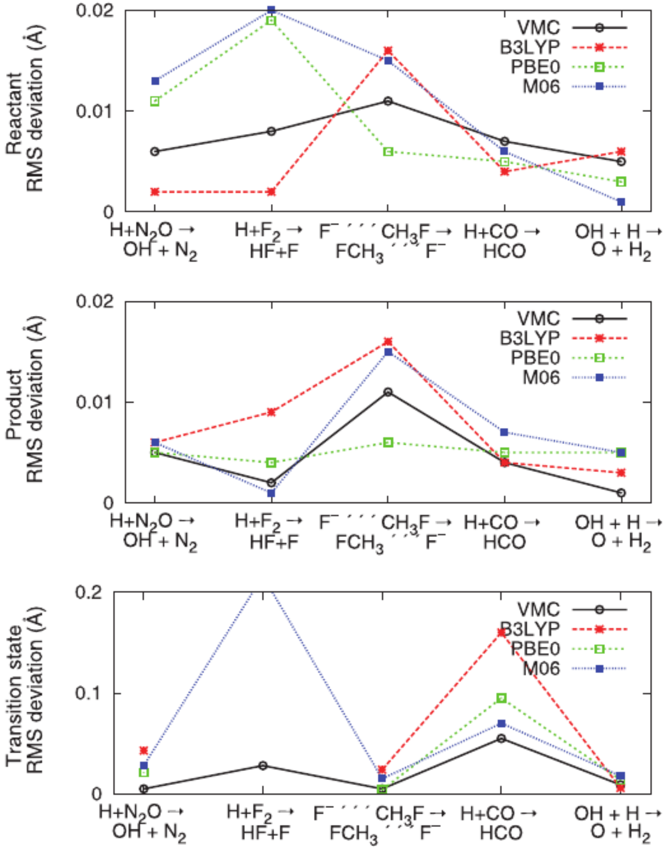

- QMC marginally better for reactants and products
- QMC significantly better for transition states

QMC vs DFT energies

	MUD
VMC	4.5
DMC	0.4
B3LYP	3.1
PBE0	2.0
M06	0.7

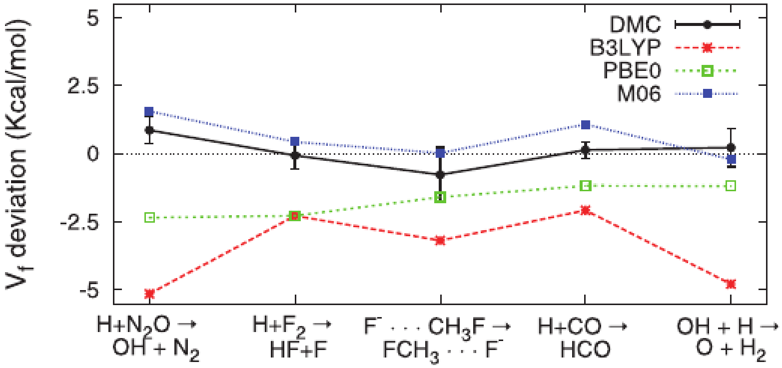

Forward barrier

VMC	8.1
DMC	3.0
B3LYP	5.2
PBE0	5.9
M06	3.5

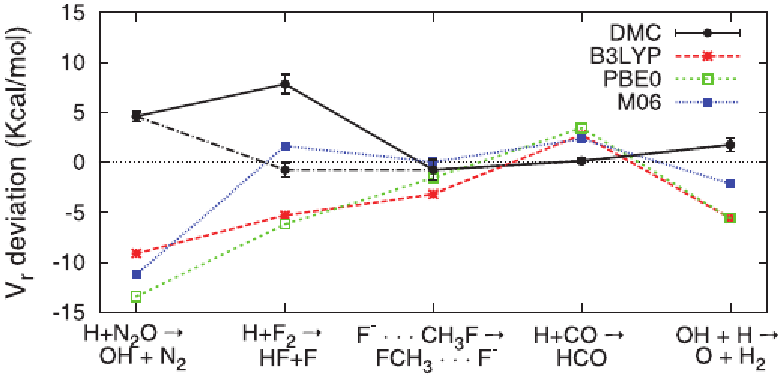

Reverse barrier

- DMC ~ M06

QMC vs DFT energies

	MUD
VMC	4.5
DMC	0.4
B3LYP	3.1
PBE0	2.0
M06	0.7

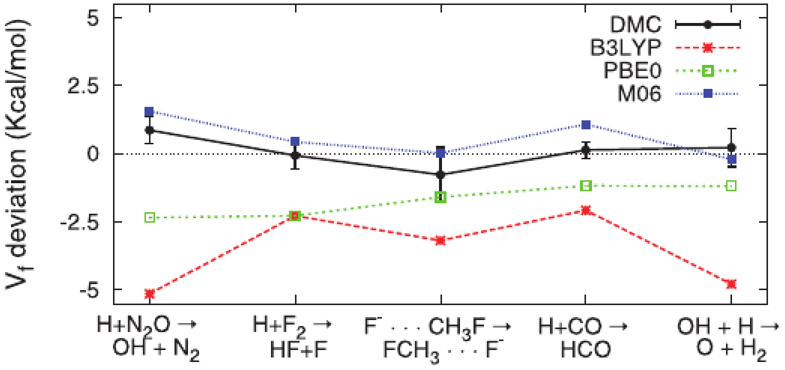

Forward barrier

VMC	8.1
DMC	3.0 (1.8)
B3LYP	5.2
PBE0	5.9
M06	3.5

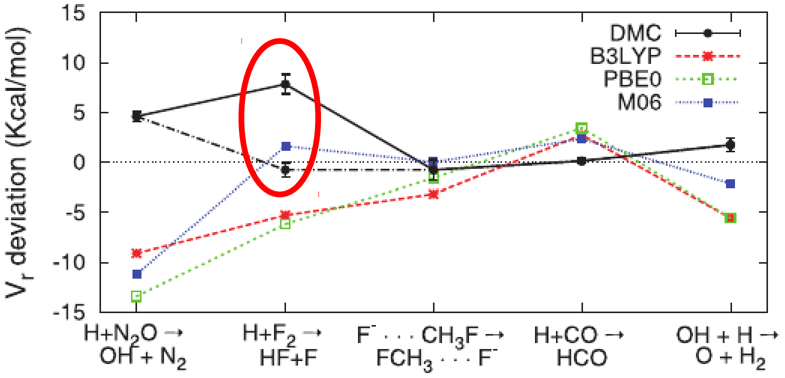

Reverse barrier

- DMC ~ M06
- DMC improves with a small CAS (~ten determinants)

- ✓ Presumably scalable (algorithmic differentiation, large optimizations):

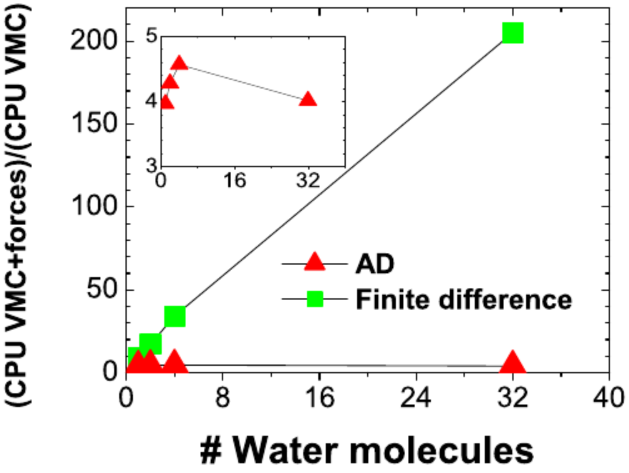

S.Sorella and L. Capriotti,
JCP 133, 234111 (2010)

extra factor in CPU time to compute forces independent of the number of atoms

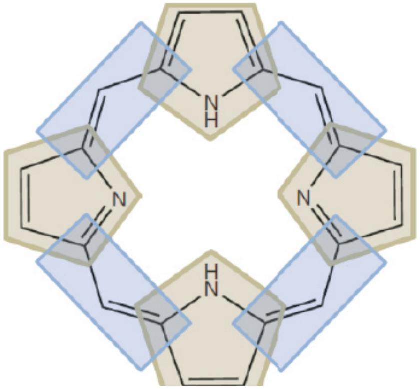

free base porphin

E.Neuscamman, C.Umrigar, and G. Chan,
PRB 85, 045103 (2012)

optimization of ~10,000 variational parameters

Improving the trial function: iterative backflow

(Markus Holzmann)

- backflow defines dressed particles with renormalized coordinates and weaker correlations

$$\mathbf{q}_i = \mathbf{r}_i + \sum_j \eta(r_{ij})(\mathbf{r}_i - \mathbf{r}_j), \qquad D = \det(\phi_i(\mathbf{q}_j))$$

- dressed particles can still be viewed as a Fermi liquid, and backflow transormation can be iterated:

$$\Psi_{BF0} = J_0(R)D(Q_0)$$

$$\Psi_{BF1} = J_0'(R)J_1(Q_0)D(Q_1)$$

$$\Psi_{BF2} = J_0''(R)J_1'(Q_0)J_2(Q_1)D(Q_2)$$

$$\cdots\cdots$$

- Non-interacting nodes in the n-th renormalized coordinates become more and more accurate.

- Ithe computational cost of iterative backflow remains $\propto N^3$
- backflow can be used for other wave functions (geminals, pfaffians, compete-active-space, ...)

Results: fixed-node energies with various nodes (PW, BF0, BF1, BF2, BF3) and unbiased energy (TE) for 2D 3He at freezing density (Aziz potential)

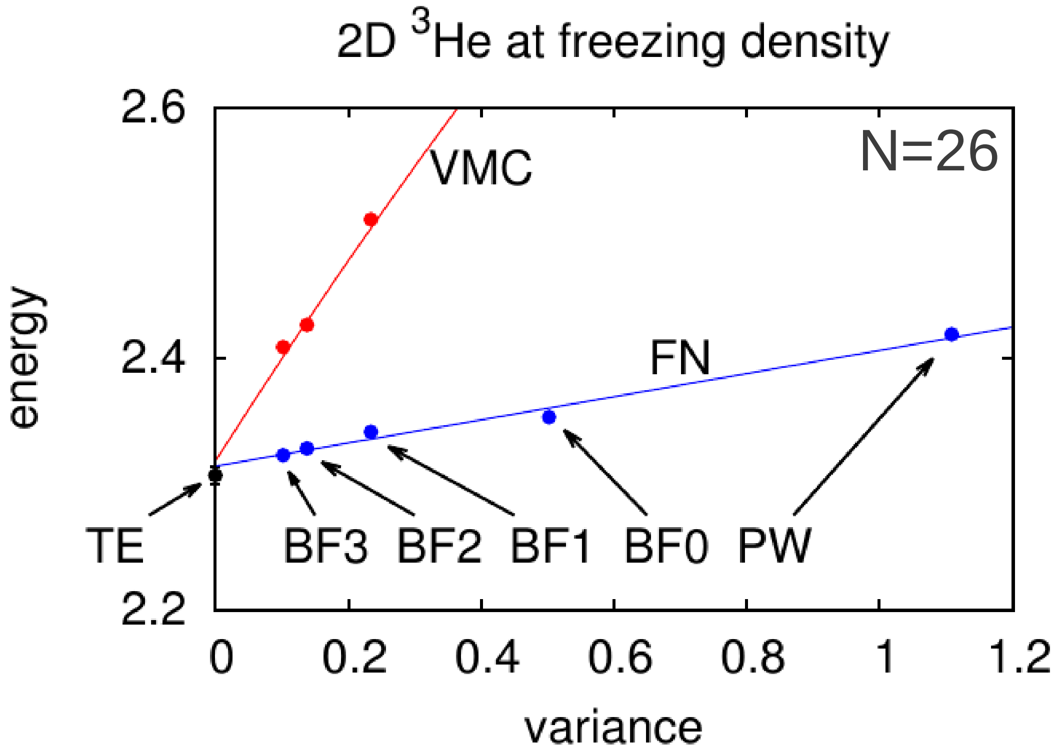

Summary part 1

- NEB calculation with full QMC forces reasonably automatic and stable

- Based on a few reactions:
  - VMC geometry improves DFT results
  - DMC energy at least as good as M06 with simple SJ wavefunctions

- At this level of accuracy, presumably scalable to large systems

- Improvements possible in specific situations using better wavefunctions

2) imaginary-time correlation functions: unbiased fermionic energies, static and dynamic response

Linear static response can be obtained from energy derivatives:

$$H = H_0 + 2\lambda_{\mathbf{q}} \sum_i \cos(\mathbf{q} \cdot \mathbf{r}_i)$$

perturb the hamiltonian with an external field

$$\chi(q) = d^2 E(\lambda, q)/d\lambda^2$$

static susceptibility

an example:
2D electron gas at rs=5

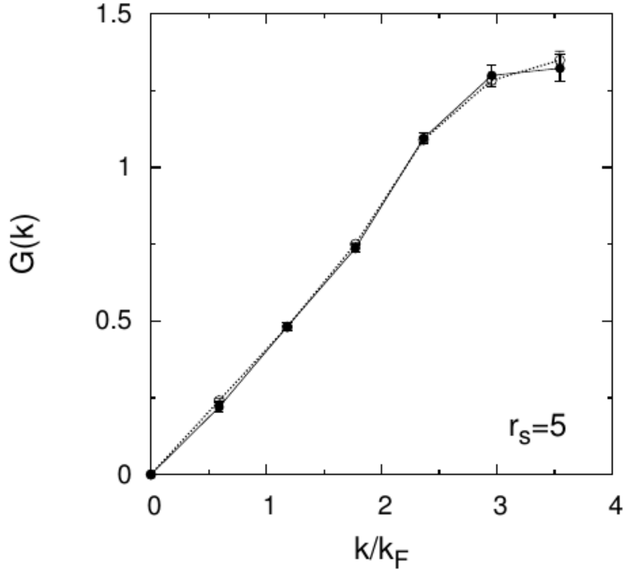

$$G(q)v(q) = 1/\chi(q) - 1/\chi_0(q) + v(q)$$

Drawback: we need to optimize
the dependence of the trial function
on the external field(s).

Linear static response from imaginary-time correlation functions:

$$F(q,\tau) = \langle \rho_q(\tau)\rho^{\dagger}_{-q}(0)\rangle / N_P \qquad \rho_q = \sum_i \exp(-i\mathbf{q}\cdot\mathbf{r}_i)$$

$$\chi(q) = -2\int_0^{\infty} d\tau\, F(q,\tau)$$

4He at equilibrium density

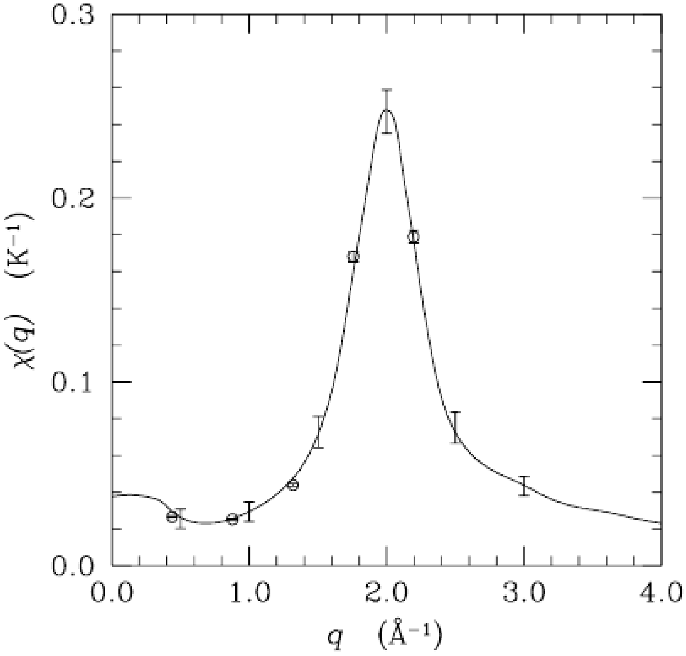

straightforward for bosons

Linear static response from imaginary-time correlation functions:

2D jellium, rs=5

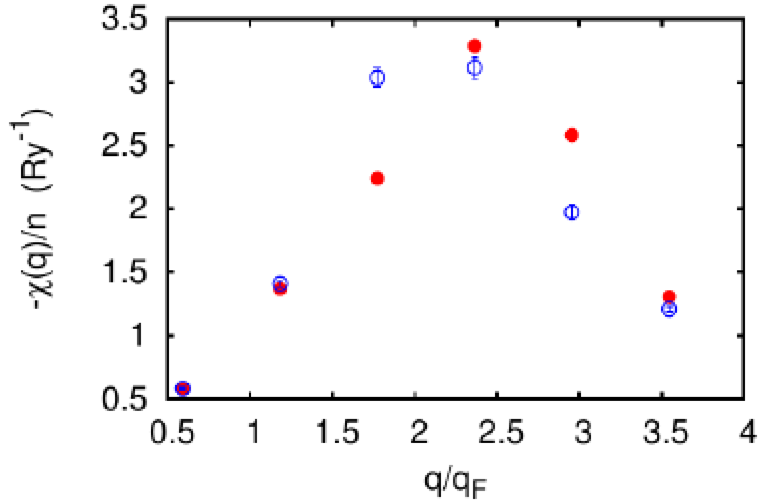

Non interacting

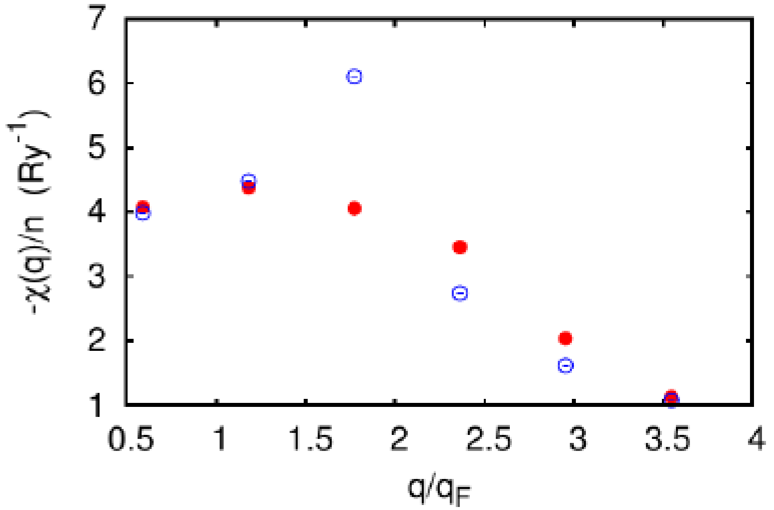

Φ From fixed-node $F(q, \tau)$

● “exact”

Fixed-node is poor for imaginary-time correlations, regardless of the quality of the trial function.

a different nodal constraint: phaseless AFQMC [S.Zhang and H.Krakauer, PRL 90, 136401 (2003)]

- Hubbard-Stratonovich transformation maps many-body propagator into one-body propagator with fluctuating auxiliary fields
- Imaginary time evolution simulated by a random walk in the space of Slater determinants

- Importance sampling enhances overlap between random walker $|\phi\rangle$ and trial function $|\Psi_T\rangle$
- Phaseless approximation: branching weight approximated by

$$\exp(-\tau \mathrm{Re}[E_L(\phi)])$$

➔ Very good results for ground-state energy even with poor trial functions

How good for imaginary-time correlation functions?

$F(q,\tau)$ for 2D jellium (N=2)

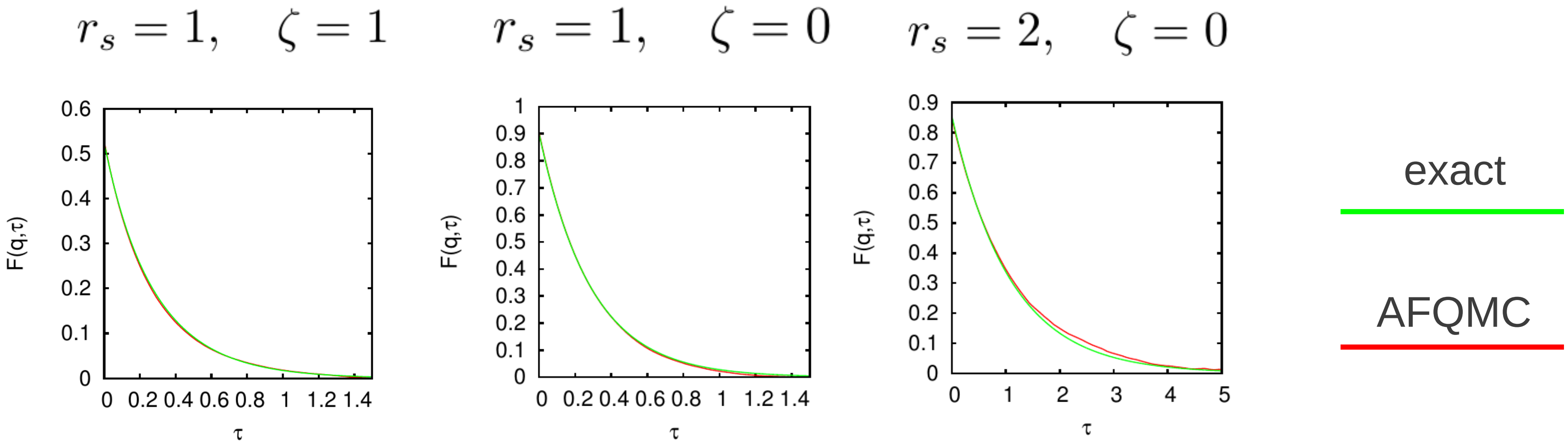

- Phaseless AFQMC looks good for imaginary-time correlations yet another nodal constraint: restricted path (Ceperley)

Test: non-interacting fermi gas (here restricted path should be exact).

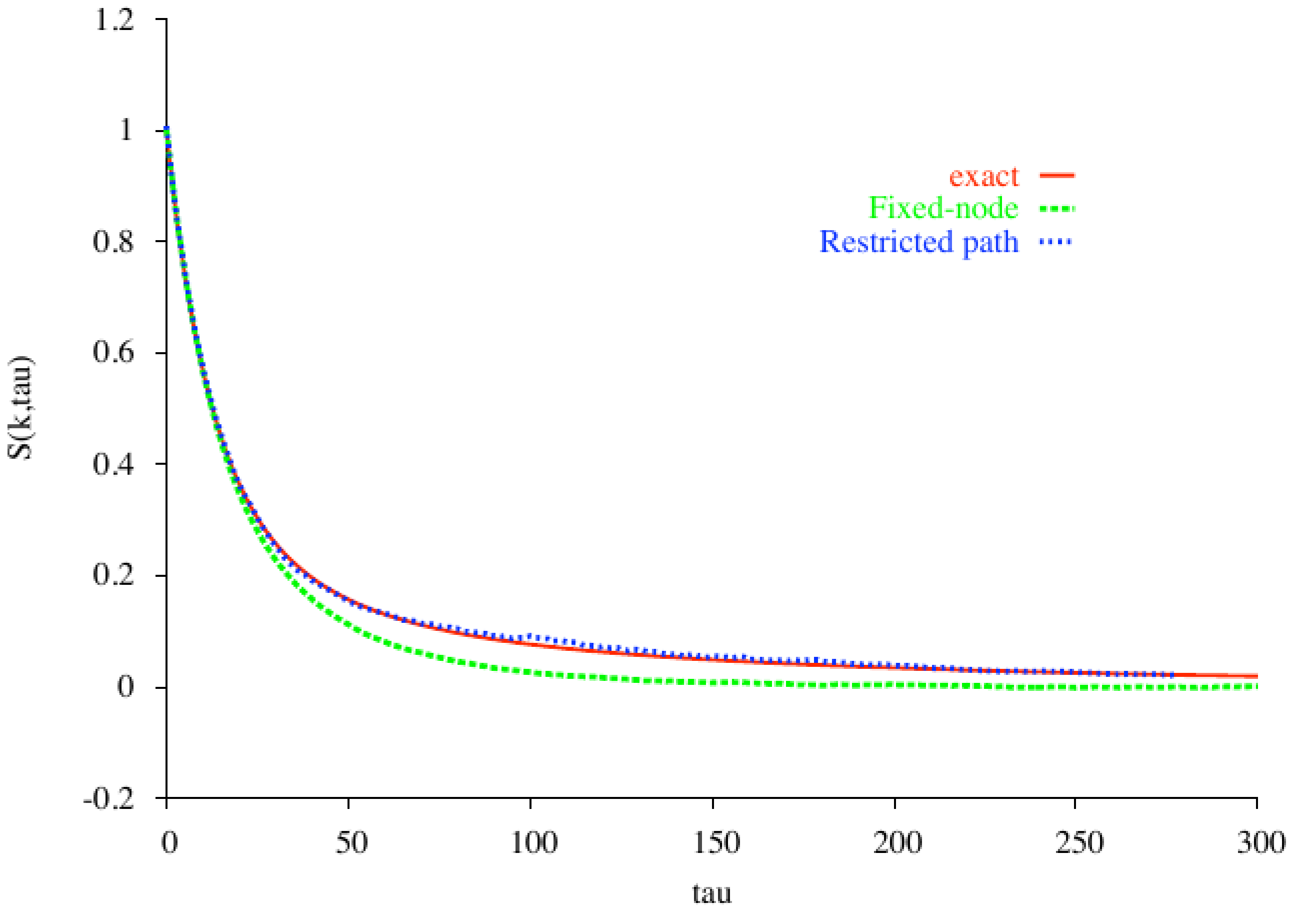

yet another nodal constraint: restricted path (Ceperley)

Test: **2D electron gas: r_s=10 (N=26):**

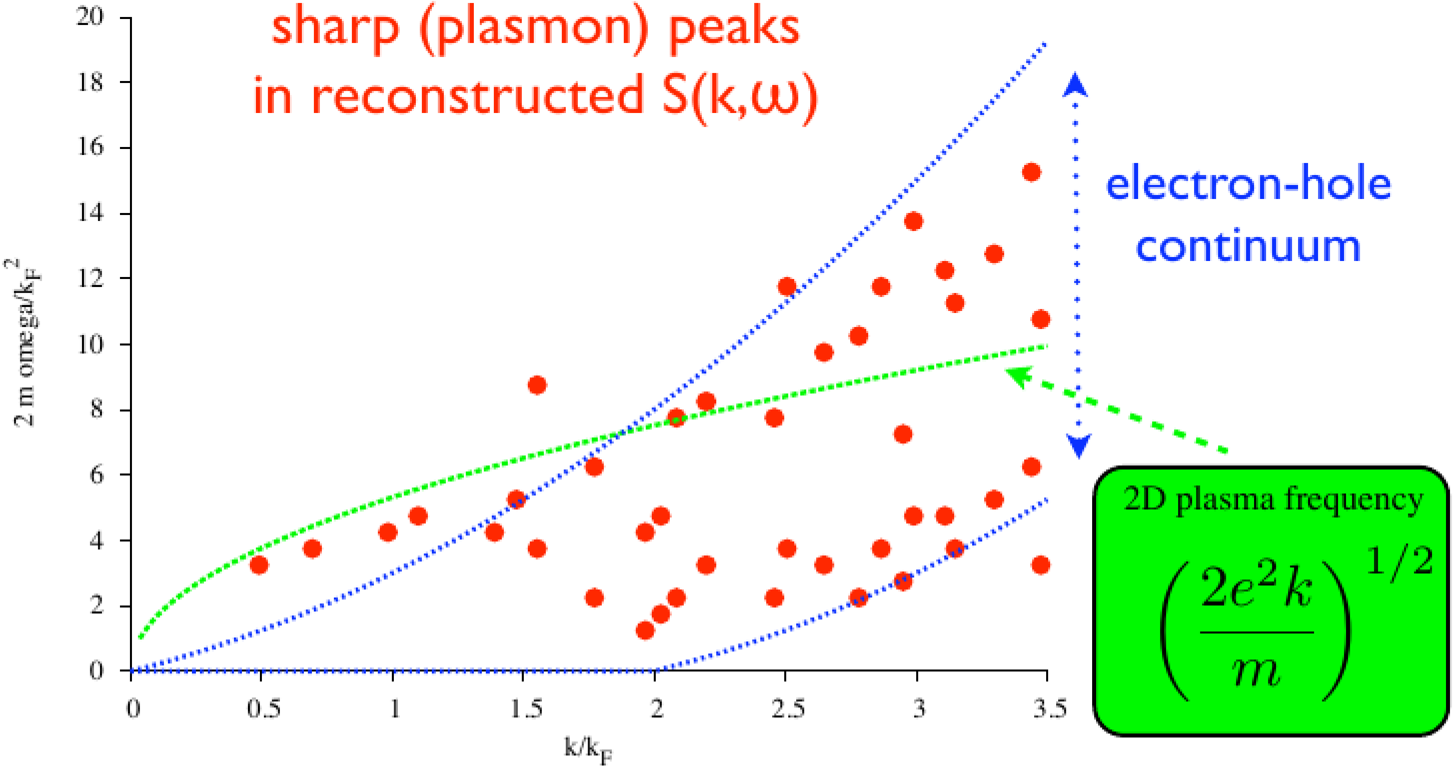

sharp (plasmon) peaks in reconstructed S(k,ω)

electron-hole continuum

2D plasma frequency

$$\left(\frac{2e^2k}{m}\right)^{1/2}$$

Fermionic states as excitations from the bosonic ground state:

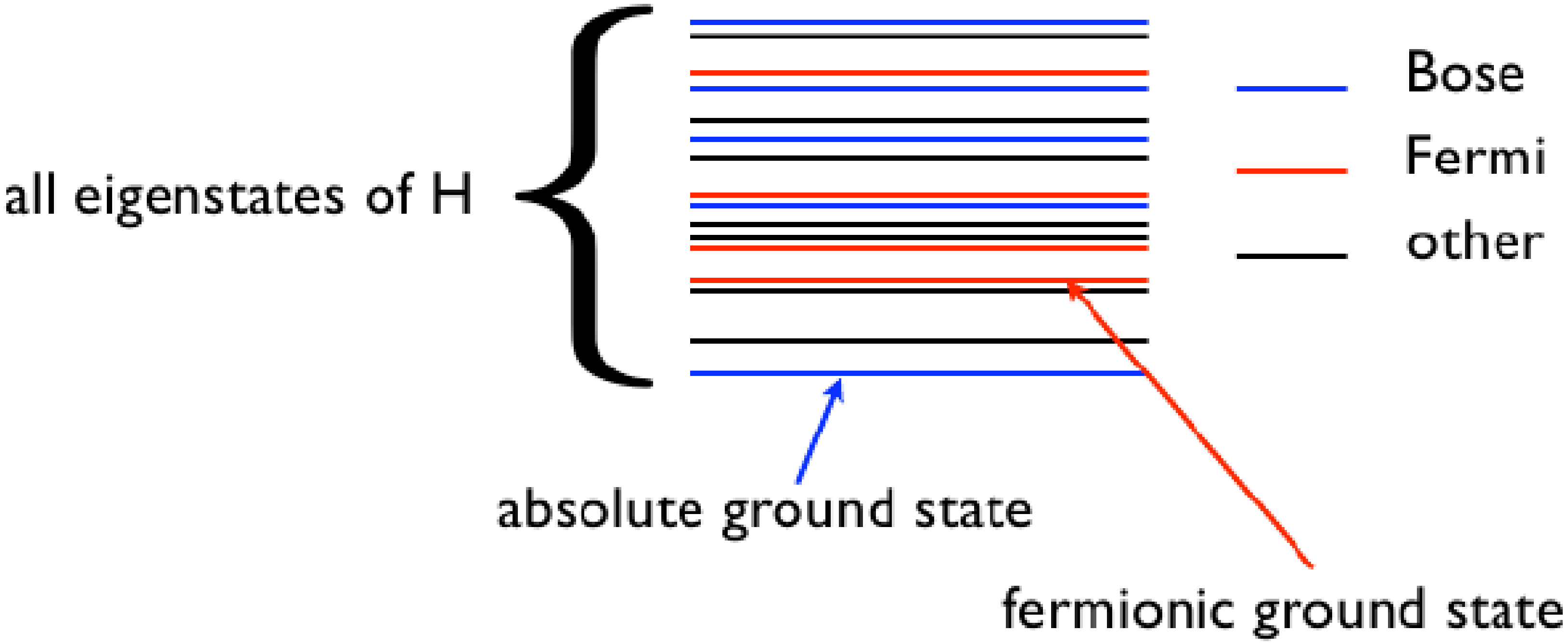

$$c(\tau) = \langle D e^{-\tau H} D^* \rangle = \sum_i |\langle \Phi_0 | D | \Psi_i \rangle|^2 e^{-\tau E_i}$$

Φ_0 bosonic ground state; Ψ_i , E_i Fermionic eigenstates/values

$\langle \cdot \rangle$ is the expectation value on the bosonic ground state

$$c(\tau) = \langle D e^{-\tau H} D^* \rangle = \sum_i |\langle \Phi_0 | D | \Psi_i \rangle|^2 e^{-\tau E_i}$$

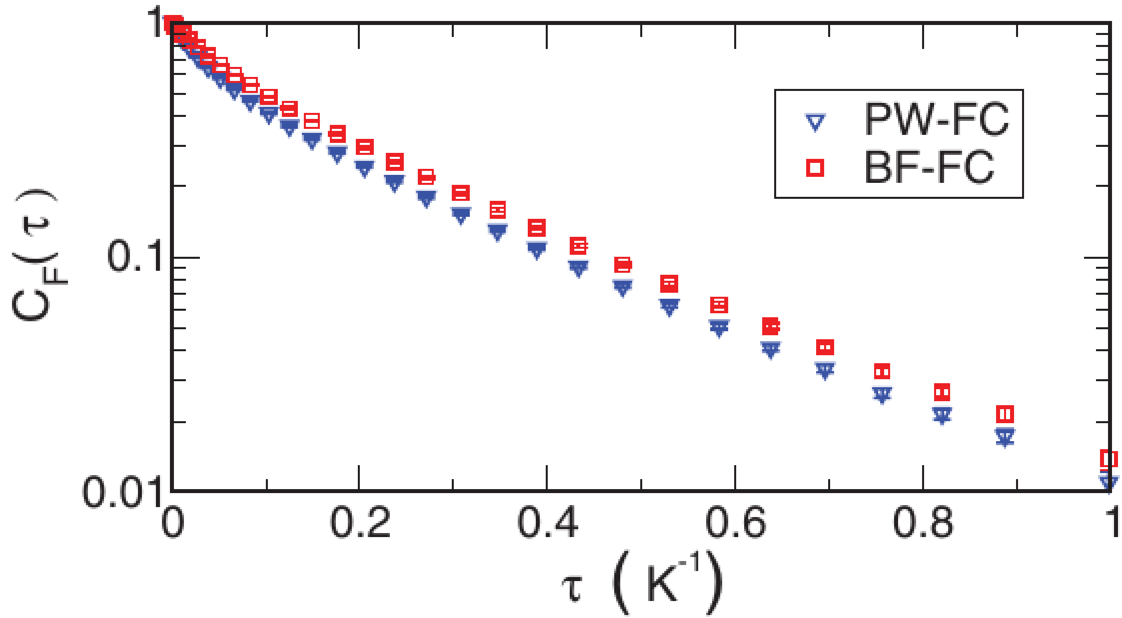

The long-time exponential decay of the correlation function gives E_0

Results using either plane-wave or backflow in D are consistent

Like TE, this method works if the Fermi-Bose gap (order N) is not much larger than the first fermionic excitation (order 1)...

Unlike TE, this method does not need to divide by the average sign

Spin susceptibility (from a quadratic fit to $E(\zeta)$ in [0,1])

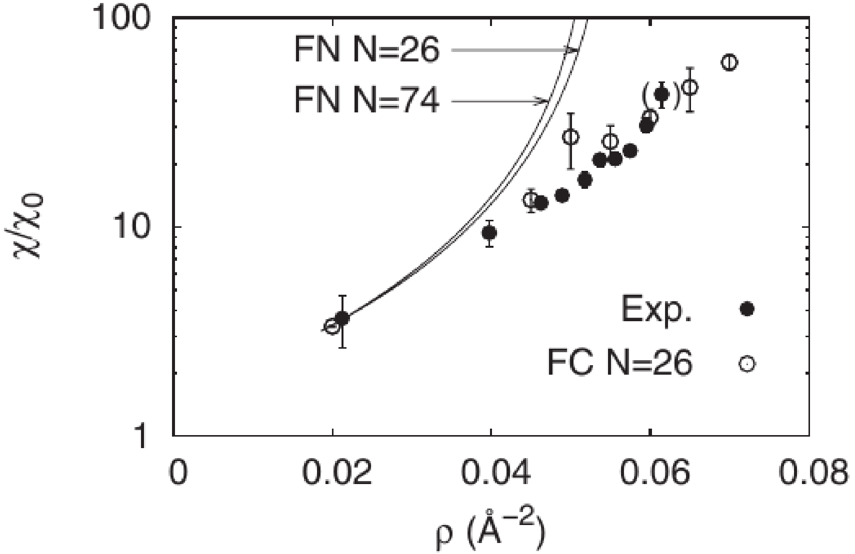

FIG. 7. Enhancement of the spin susceptibility as a function of the density: (filled circles) as measured in the second layer of ^3He on graphite[2]; (open circles) as calculated assuming a quadratic dispersion over the whole polarization range in Fig. 6. The corresponding Fixed-node result from Fig. 5 would diverge at $\rho \simeq 0.050$ Å^{-2}.

dynamic structure factor

$$F(q,\tau) \simeq \frac{\langle D(\tau)\rho_q(\tau)\rho_{-q}(0)D^*(0)\rangle}{\langle D(\tau)D^*(0)\rangle}$$

- Numerator and denominator computed as expectation values on the Bosonic ground state $|\Phi_0\rangle$.
- The exact Fermionic ground state $|\Psi_0\rangle$ is replaced by $D|\Phi_0\rangle$.
- While for the Fermionic ground state it is sufficient to identify the exponential tail of the correlation function, for the Fermionic spectrum a full inverse Laplace transform of $F(q,\tau)$ is needed.

$$F(q,\tau) = \int d\omega e^{-\omega\tau} S(q,\omega)$$

inverse Laplace transform with the GIFT algorithm (E. Vitali et al. 2010).

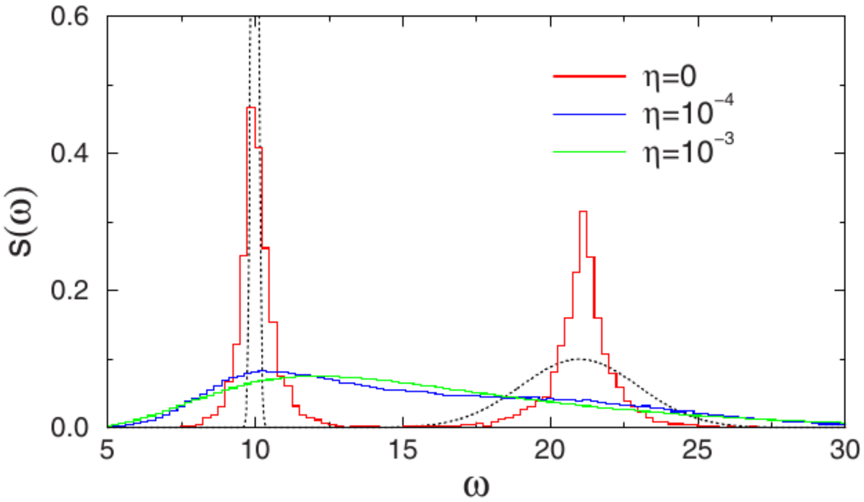

Maximum Entropy vs. GIFT (genetic inversion via falsification of theories).

GIFT gives more structure in the reconstructed spectrum.

Results: dynamic structure factor of 2D 3He

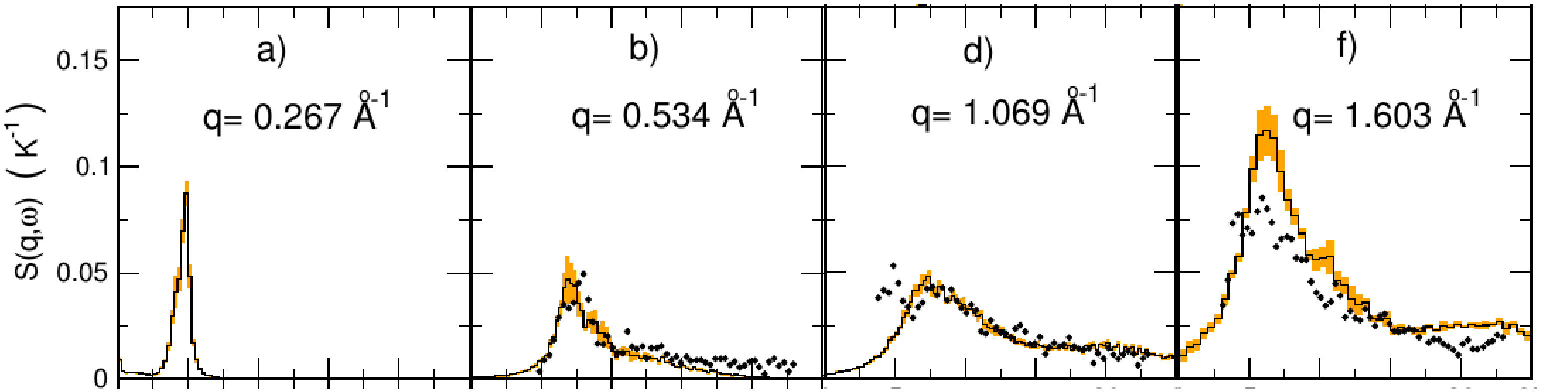

Histograms with errorbars: simulation; points: experiment

Summary part 2: imaginary-time correlations for fermions

With nodal restrictions:

- Avoid the fixed-node approximation
- Phaseless AFQMC OK
- Restricted path OK

Without nodal restriction:

- A slightly different TE algorithm
- Good results for dynamic structure of 3He